Quaternary Research 78 (2012) 513–527

Contents lists available at SciVerse ScienceDirect

Quaternary Research

journal homepage: www.elsevier.com/locate/yqres

Major hydrological regime change along the semiarid western coast of South America during the early Holocene

Cristina Ortega [a,*], Gabriel Vargas [a], José A. Rutllant [b,c], Donald Jackson [d], César Méndez [d]

[a] Departamento de Geología, Facultad de Ciencias Físicas y Matemáticas, Universidad de Chile, Plaza Ercilla 803, Santiago, Chile
[b] Departamento de Geofísica, Facultad de Ciencias Físicas y Matemáticas, Universidad de Chile, Blanco Encalada 2002, Santiago, Chile
[c] Centro de Estudios Avanzados en Zonas Áridas, Raúl Bitrán s/n, Colina El Pino, La Serena, Chile
[d] Departamento de Antropología, Facultad de Ciencias Sociales, Universidad de Chile, Ignacio Carrera Pinto 1045, Santiago, Chile

ARTICLE INFO

Article history:
Received 30 December 2011
Available online 8 September 2012

Keywords:
Paleoclimate
Early Holocene
Alluvial flow
Heavy rainfall
Coastal fog
El Niño Southern Oscillation (ENSO)
Western South America
Paleohydrology
Pacific Ocean

ABSTRACT

Water availability in the semiarid western coast of Chile (30–32°S) is conditioned by high interannual precipitation variability, reflecting the transition between arid subtropical and moist mid-latitude climates in the Southeastern Pacific Ocean. A paleoclimate reconstruction based on the latest Pleistocene–Holocene geological record from the Quebrada Santa Julia archeological site in Chile (31°50′S) and on modern meteorological mechanisms producing alluvial episodes in this region indicates a major change in the rainfall regime shortly after 8600 cal yr BP. This, together with other paleoclimate proxies along the west coast of South America (34°–14°S), suggests La Niña-like conditions 13,000–8600 cal yr BP. Based on sedimentological and geomorphologic evidence, we hypothesized that the absence of heavy rainfall events in northern Chile and the new hydrological regime that prevailed ca. 8600–5700 cal yr BP in north-central Chile resulted from an increase in the large-scale westerly flow over central Chile, as expected in near-neutral ENSO conditions. This atmospheric circulation anomaly is compatible with an equatorward shift of the influence of the Southeast Pacific Subtropical Anticyclone relative to the early Holocene, prior to the onset of modern ENSO variability.

Introduction

Variations in the hydrologic regime along tropical and subtropical continental margins depend strongly on changes in regional ocean-climate conditions. Major climate changes during the latest Pleistocene–Holocene period have been suggested along the subtropical Southeast Pacific from paleoceanographic inferences (Kim et al., 2002; Kaiser et al., 2005; Ortlieb et al., 2011) and continental records (Sandweiss et al., 1996; Rodbell et al., 1999; Moy et al., 2002; Vargas et al., 2006). Nowadays, there is a general agreement respect to the onset of El Niño-Southern Oscillation (ENSO) manifestations along the west coast of South America at 5500–5300 cal yr BP, which has been related to tropical ocean–atmosphere mechanisms (e.g. Rodbell et al., 1999) triggering the present tropical–extratropical atmospheric teleconnections (e.g. Vargas et al., 2000, 2006). Nevertheless, the impact of latest Pleistocene–early Holocene ocean-climate changes on hydrologic regime variations along the subtropical western margin of South America, which includes the semiarid coast of Chile (30–32°S), is still uncertain.

Pollen records from the semiarid coast of Chile (31°50′–32°S; Maldonado and Villagrán, 2006; Maldonado et al., 2010) have suggested wetland expansions with dry phases during the early Holocene and arid conditions during the mid-Holocene. In central Chile, sedimentary and pollen records from Aculeo Lake (33º50′S; Jenny et al., 2002) also indicate arid conditions during the mid-Holocene, and even drier conditions during the early Holocene (9500–8500 cal yr BP). Oceanographic records offshore 33°S (Kim et al., 2002) and 30°S (Kaiser et al., 2005) show cold conditions prior to the Holocene. To explain such climate changes, latitudinal variations on the position and strength of the mid-latitude westerlies and Southeast Pacific Subtropical Anticyclone (SEPSA) at latest Pleistocene–Holocene time scale have been suggested (Heusser, 1990; Villagrán and Varela, 1990; Veit, 1996; Grosjean et al., 1997; Lamy et al., 1999, 2002; Jenny et al., 2002, 2003; Villa-Martínez et al., 2003; Maldonado and Villagrán, 2006; Vargas et al., 2006; Maldonado et al., 2010). Further, prevailing La Niña-like conditions have been proposed during the early Holocene (Vargas et al., 2006), and during the middle Holocene (Kaiser et al., 2005; Carré et al., 2011).

Because of its location in the transition zone between the hyperarid Atacama Desert and wetter mid-latitude climates, the semiarid coast of Chile is a sensitive region for the study of hydrologic variations related to ocean-climate changes. This research focuses on paleoclimate reconstruction and the hydrologic behavior of this region during the latest Pleistocene and Holocene periods, through the geomorphologic analysis of Los Vilos area (31°50′S; Fig. 1), together with chronostratigraphic and sedimentological study of the Quebrada Santa Julia (QSJ) archeological site (Jackson et al., 2007). A historical record of debris-flow occurrence and flooding events was created by analyzing heavy rainfall episodes in the area since

* Corresponding author.
E-mail address: crortega@ing.uchile.cl (C. Ortega).

0033-5894/$ – see front matter © 2012 University of Washington. Published by Elsevier Inc. All rights reserved.
http://dx.doi.org/10.1016/j.yqres.2012.08.002

1950, their associated atmospheric circulation patterns and geological effects. From this combined geomorphologic, historical and meteorological study, we propose changes in the hydrologic regime and climate conditions since 13,000 cal yr BP in the QSJ site region. The comparison of our findings with previous paleoclimate and paleoceanographic results in the tropical–subtropical Southeast Pacific region indicates a change from prevailing La Niña-like conditions before 8600 cal yr BP to neutral conditions followed by the onset of modern El Niño variability since the mid-Holocene.

Climate and geomorphologic setting

The transition climate of the semiarid coast of Chile lies at the southern edge of the Atacama Desert, whose hyperaridity is strongly associated to the quasi-permanent influence of the Southeast Pacific Subtropical Anticyclone (SEPSA), to low coastal sea-surface temperatures (SSTs) and regional atmospheric circulation features associated with the daily cycle of insolation along the western slope of the Andes (Rutllant et al., 1998; Strub et al., 1998; Fig. 1). Most of the rainfall in this climate transition zone occurs during austral winter associated with the seasonal drift of the mid-latitude westerlies, with annual mean values of 80 mm at 30°S, 180 mm at 32°S and 380 mm at 33°S (Fig. 1). Cold conditions in the coastal ocean are associated with the Humboldt Current System, which drives subantarctic waters equatorward, and with coastal upwelling processes which strengthen the high atmospheric stability associated with the SEPSA (Rutllant et al., 1998; Strub et al., 1998). This subtropical regime favors the persistence of stratus clouds over the ocean, especially during austral spring

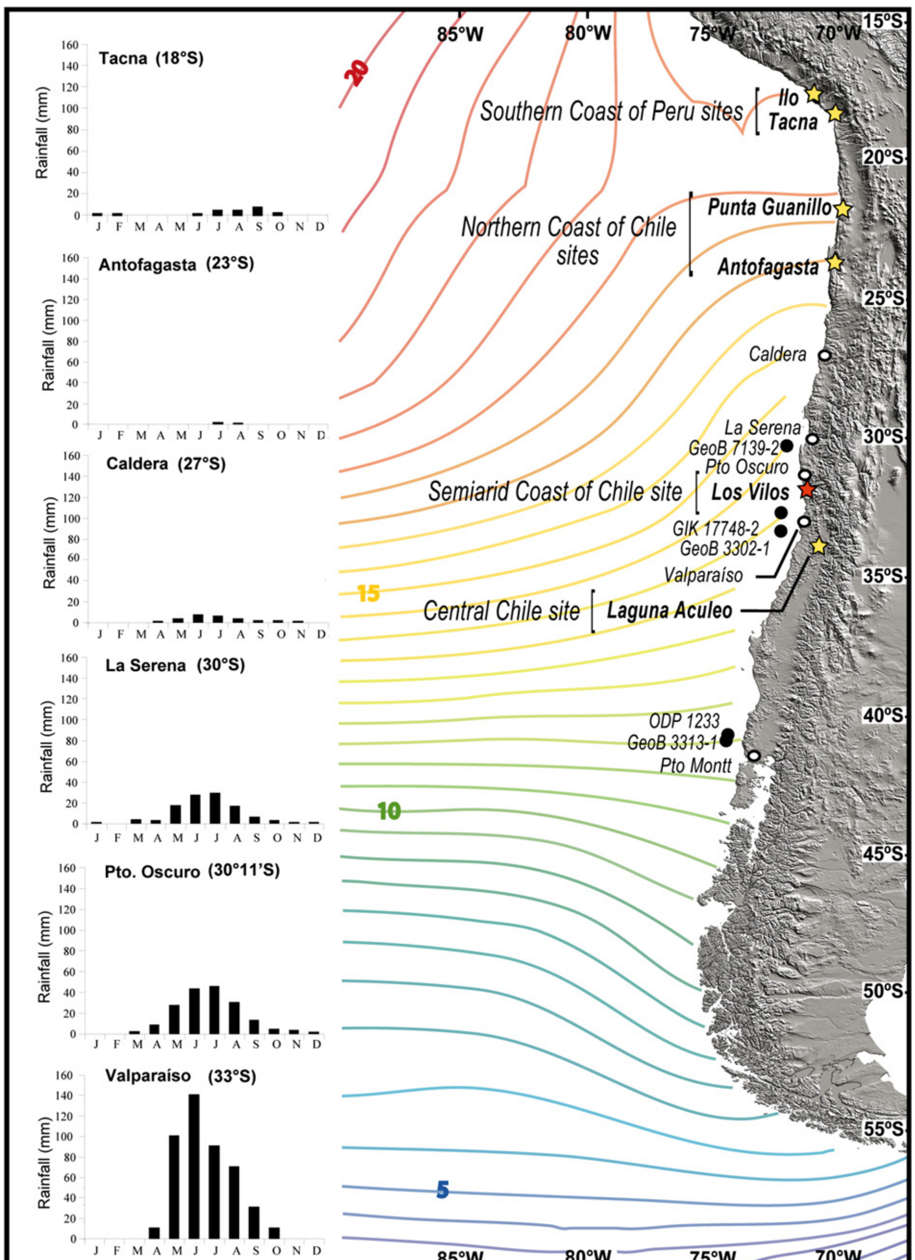

Figure 1. Geomorphological setting of the different sites considered in this work. Location of the paleoclimatic record proposed in this work (red star), continental records (yellow stars), marine cores (black circles) and meteorological stations (white circles). Graphics of monthly rainfalls during 1950–2000 show the latitudinal distribution of precipitation along coastal Chile. Sea surface temperature from NOAA extended SST data over winter–spring season (June to November).

https://doi.org/10.1016/j.yqres.2012.08.002 Published online by Cambridge University Press

(Rutllant et al., 1998; Garreaud et al., 2008), creating elevated fogs whenever these clouds intercept the coastal mountain range.

The QSJ site is located 5 km northeast of Los Vilos (31°50′S; Fig. 1), within the NE–SW oriented Mal Paso ravine which is the main stream of a 16 km^2 hydrographic basin surrounded by dunes (Fig. 2). This geomorphologic setting makes this place suitable to record the occurrence of heavy rainfall events, in which the downstream sand transport is favored. Currently, the Mal Paso ravine ends in the Pacific Ocean, but according to geomorphologic analyses and archeological data the ravine was blocked by dunes during the latest Pleistocene, particularly between 16,000 and 13,000 cal yr BP (Fig. 2, Table 1 and Supplementary information). This geomorphologic feature produced a local base level which favored alluvial sedimentation upstream, driving the formation of a 10 m thick alluvial sequence characterized mostly by sandy and fine gravel deposits. The beginning of the incision of the hydric system, associated with the filling of the local basin and to a hydrologic change, generated the abandonment of the previous sedimentary unit, resulting in the formation of the oldest alluvial terrace in the ravine (AT3; Fig. 2). During the incision process two lower alluvial terraces (AT2 and AT1; Fig. 2) associated with coarse gravel and breccia deposits were formed as the result of episodic aggradation and downcutting through the blocking dunes. As the incision prevailed along the contact between AT3 and the paleodunes (Fig. 2), most of the alluvial unit was preserved. Here, we interpret paleohydrologic and paleoclimate changes from the sedimentary record constituting the geomorphologic units in the area of QSJ site, supported by the analysis of modern climate scenarios explaining the occurrence of historic alluvial episodes in the region.

Methods

The geomorphologic and morpho-stratigraphic study was performed through the analysis of aerial photographs (1:30,000), satellite images (25 and 28.5 m/pixel), topographic and bathymetric charts (1:50,000), digital elevation models and detailed chronostratigraphic columns and sedimentological characterization. This resulted in a local geomorphologic map of the QSJ site area (1:25,000; Fig. 2).

The geochronological models are based on twelve radiocarbon ages from QSJ site and on thirteen ages performed through different techniques from archeological sites in the surrounding dunes (see Table 1). At the QSJ site, eight previous ages (Jackson et al., 2007; Méndez et al., 2007) together with four new ages were used for paleoclimate reconstructions of the alluvial sequence constituting AT3 (Figs. 2 and 3). Four dates from the latest Pleistocene human occupation level provided an age for the base of the paleoclimate record. The other radiocarbon results

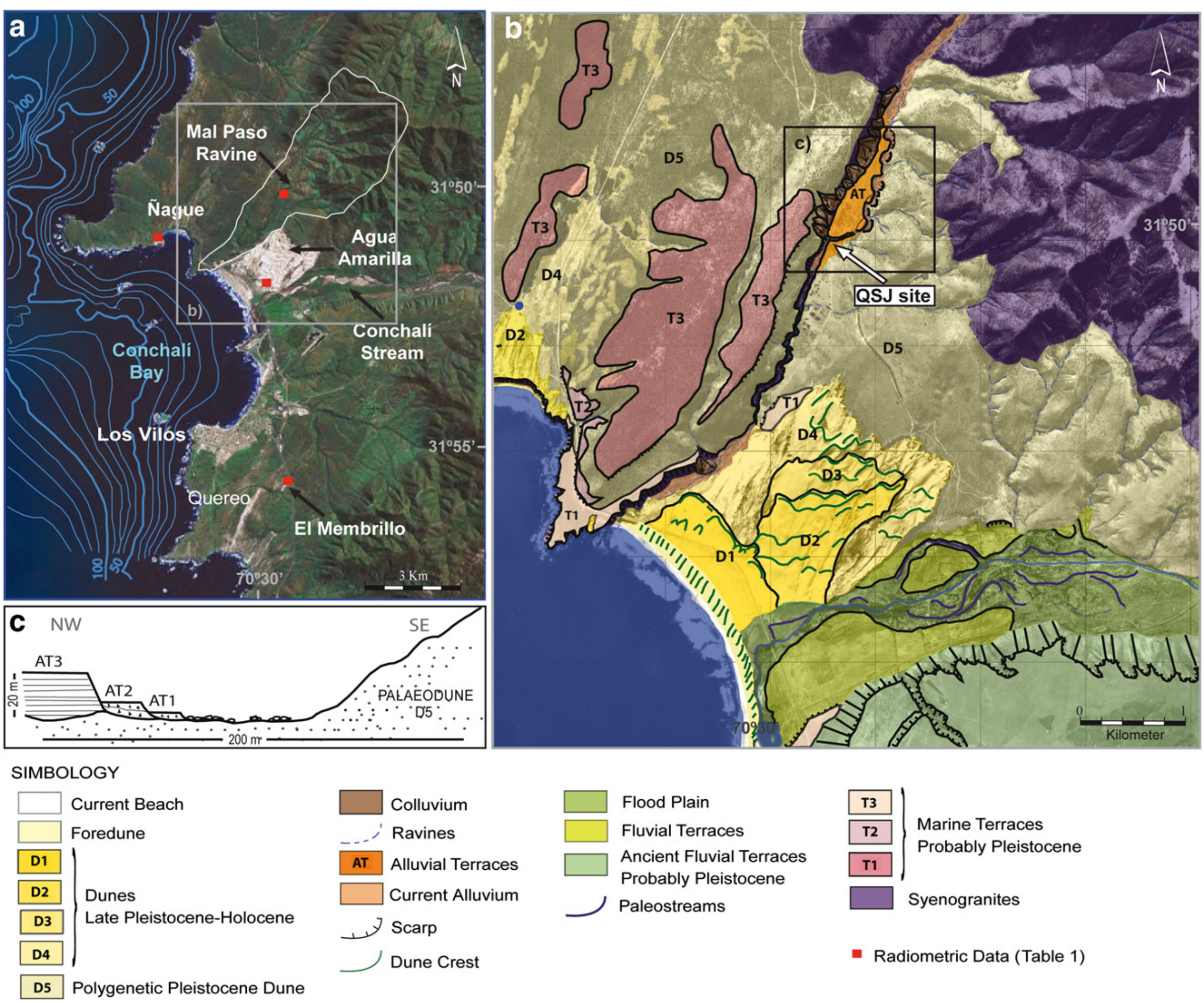

Figure 2. Geomorphological setting of the study area (Los Vilos, semiarid coast of Chile). a) Satellite image showing radiometric data from archeological sites and bathymetric curves (each 10 m); b) geomorphological map (1:25.000). The paleoclimatic record is located at the alluvial terraces colored in orange. c) Schematic configuration of the three alluvial terraces (AT3, AT2 and AT1). See Table 1 for radiometric data from geomorphological unit.

https://doi.org/10.1016/j.yqres.2012.08.002 Published online by Cambridge University Press

Table 1
Chronological data from Los Vilos area.

Unit	Archeological site	Material	Laboratory number	Age, ^{14}C yr BP	Mean calibrated age, cal yr BP	Calibrated age range, (2σ), cal yr BP	Reference
Radiocarbon, AMS							
Alluvial terrace AT3	LV.221	Clayey mud	Beta 216693	2690 ± 40	2805	2860–2750	Méndez et al. (2007)
Alluvial terrace AT3	LV.221	Clayey mud	Beta 243478	3680 ± 40	4000	4100–3900	This work
Alluvial terrace AT3	LV.221	Clayey mud	Beta 243479	3780 ± 40	4020	4040–4000	This work
Alluvial terrace AT3	LV.221	Clayey mud	Beta 243480	3780 ± 40	4165	4250–4080	This work
Alluvial terrace AT3	LV.221	Clayey mud	Beta 243481	5140 ± 40	5910	5940–5880	This work
Alluvial terrace AT3	LV.221	Clayey mud	Beta 20523	7830 ± 40	8595	8660–8530	Jackson et al. (2007)
Alluvial terrace AT3	LV.221	Clayey mud	Beta 204524	9640 ± 50	10,965	11,180–10,750	Jackson et al. (2007)
Alluvial terrace AT3**	LV.221	Peat	Beta 196068	10,120 ± 50	11,810	12,270–11,350	Jackson et al. (2007)
Alluvial terrace AT3*	LV.221	Hearth charcoal	Beta 194725	10,920 ± 50	13,005	13,130–12,880	Jackson et al. (2007)
Alluvial terrace AT3*	LV.221	Wood instrument	Beta 215090	11,060 ± 80	13,035	13,190–12,880	Jackson et al. (2007)
Alluvial terrace AT3*	LV.221	Hearth charcoal	Beta 215089	11,090 ± 80	13,115	13,350–12,880	Jackson et al. (2007)
Alluvial terrace AT3	LV.221	Charcoal lens	Beta 202253	4200 ± 40	4720	4840–4600	Méndez et al. (2007)
Alluvial terrace AT3***	LV.221	Clayey mud	Beta 243482	7960 ± 50	8810	9000–8620	This work
Alluvial terrace AT3***	LV.221	Clayey mud	Beta 243483	9540 ± 50	10,895	11,100–10,690	This work
Dune D4 — El Membrillo	LV.105	*Mylodon* sp. verterbrae	NSRL 11081	13,500 ± 65	16,025	16,700–15,750	Jackson (2003)
Dune D2 — Ñagué	LV.098A	Shell (*Concholepas concholepas*)	NSRL 11082	11,100 ± 80	13,023	13,160–12,885	Jackson and Méndez (2005)
Radiocarbon, conventional							
Dune D2 — Ñagué	LV.098A	Shell (*Mesodesma donacium*)	Beta 94101	9,730 ± 60	11,027	11,252–10,801	Jackson and Méndez (2005)
Dune D2 — Ñagué	LV.098A	Shell (*Concholepas concholepas*)	Beta 106802	10,600 ± 70	12,601	12,806–12,396	Jackson and Méndez (2005)
Dune D2 — Ñagué	LV.098A	Shell (*Concholepas concholepas*)	Beta 55279	10,120 ± 80	11,703	12,049–11,356	Jackson (1993)
Dune D1 — Agua Amarilla	LV.166	Shell (*Concholepas concholepas*)	Beta 70246	7080 ± 60	7834	7963–7705	Jackson (2002)
Dune D1 — Agua Amarilla	LV.166	Shell (*Concholepas concholepas*)	Beta 83155	7120 ± 60	7879	8008–7749	Jackson (2002)
Unit	Archeological site	Material	Laboratory number	–	–	Age, yr	Reference
Thermoluminesence							
Dune D2 — Ñagué	LV 098A	Rock exposed to fire	UCTL 954	–	–	9550 ± 800	Roman and Jackson (1998)
Dune D1 — Agua Amarilla	LV 166	Rock exposed to fire	UCTL 980	–	–	6480 ± 325	Roman and Jackson (1998)
Dune D1 — Agua Amarilla	LV 166	Rock exposed to fire	UCTL 979	–	–	6775 ± 500	Roman and Jackson (1998)
Dune D1 — Agua Amarilla	LV 166	Rock exposed to fire	UCTL 978	–	–	6600 ± 300	Roman and Jackson (1998)
Dune D1 — Agua Amarilla	LV 166	Rock exposed to fire	UCTL 808	–	–	6800 ± 500	Roman and Jackson (1998)
Dune D1 — Agua Amarilla	LV 166	Rock exposed to fire	UCTL 749	–	–	6500 ± 500	Roman and Jackson (1998)

* Base of the late Pleistocene human occupation level.
** Roof of the late Pleistocene human occupation level.
*** Ages not considered: older than underlying strata, probably, because of reworking of old charcoal during alluvial flow.

were obtained from the overlying strata, providing a chronological framework for the estimation of the frequency of alluvial episodes during the Holocene. Conventional radiocarbon ages were obtained from Beta Analytic Inc. and calibrated using INTCAL04 (Reimer et al., 2004).

Paleoclimate interpretations were supported by the study of climate scenarios and meteorological mechanisms for the occurrence of modern heavy rainfall events, from the assessment of:

a) Historical chronicles (AD 1950–2000) concerning heavy rainfall events that resulted in debris flows and flooding episodes in the region. Data were collected from historic daily meteorological records from the Chilean Weather Service (DMC) for Puerto Oscuro and La Serena, (Fig. 1); from the newspaper "El Día" of La Serena and from "Catástrofes de Chile 1541–1992" (Urrutia and Lanza, 1993).
b) Synoptic weather conditions consisting of daily wind vectors and geopotential heights at selected pressure levels and their anomalies relative to the mean climate were obtained from the NCEP/NCAR reanalysis project (Kalnay et al., 1996).

Sedimentological record from QSJ site

The paleoclimate record consists of alluvial deposits constituting the oldest alluvial terrace AT3 (Figs. 3–5), which is 10 m high, ~1.5 km long and ~350 m wide, sitting within a latest Pleistocene paleodune system (Fig. 2; Supplementary information). The stratigraphy of the sequence constituting this terrace shows an aggradational pattern characterized by subhorizontal arrangement of the alluvial

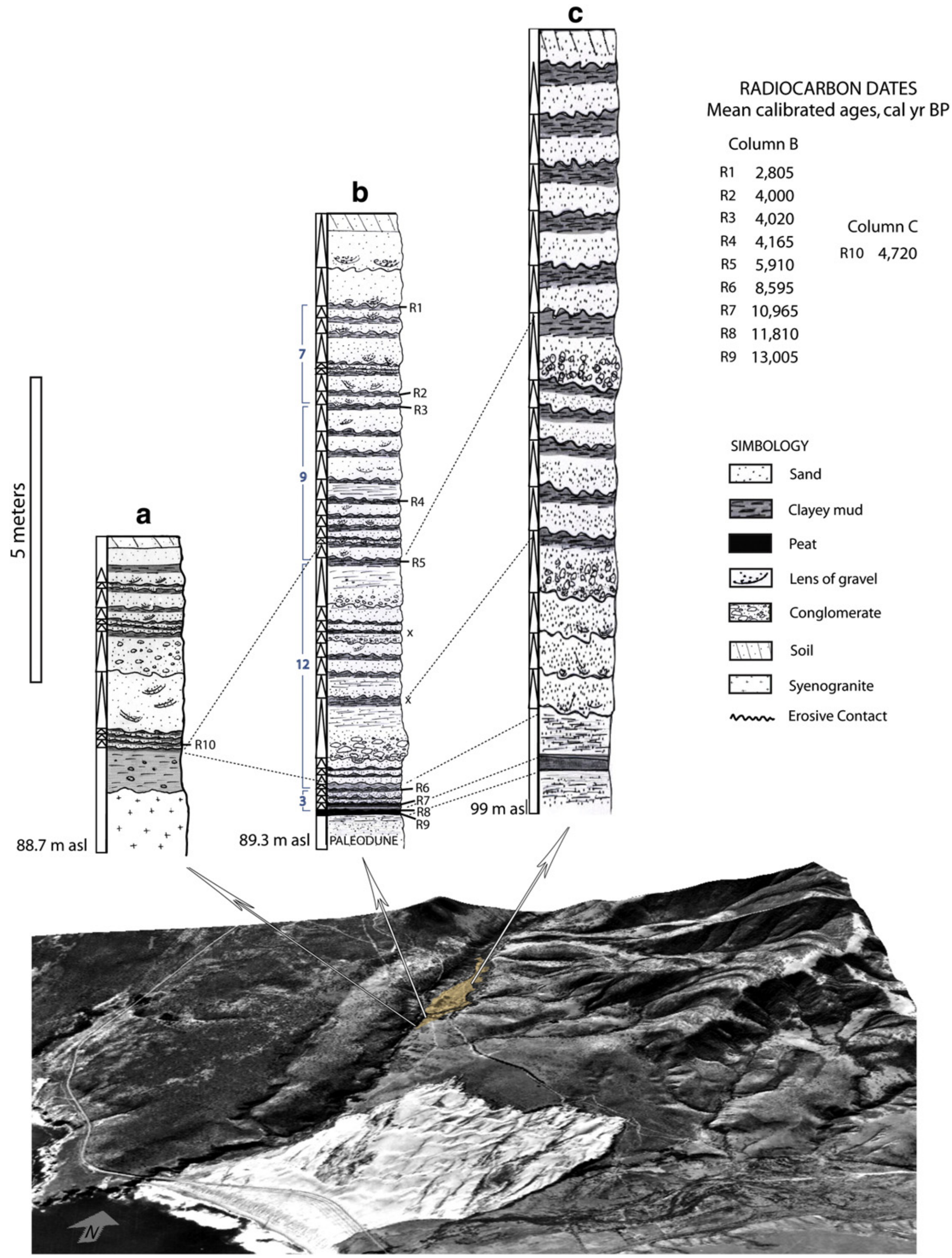

Figure 3. Sedimentology of the oldest alluvial terrace (AT3) represented by three stratigraphic columns (A, B and C) along the Map Paso ravine. The column B is located at the Quebrada Santa Julia site (black peat). The radiocarbon ages were mainly obtained from peat and clayey mud layers of this stratigraphic column. The x symbols indicate ages not considered in the geochronological model. Blue numbers indicate debris-flow events (used in Fig. 8).

strata, without any evidence of progradational deposition, like offlap contacts that could indicate filling of the local basin from headwater. Given this geometric arrangement of the alluvium, we interpret that sedimentological changes in the sequence constituting this terrace would be strictly related to hydrological factors and not to different geomorphologic conditions.

The basal exposed stratigraphy shows 40 cm of weathered sand and clay, followed by a 10 cm of black peat, where the terminal Pleistocene QSJ archeological level associated to extinct fauna consumption is located (Jackson et al., 2007). The base and top of the black peat archeological stratum have been dated at ~13,000 cal yr BP on hearth charcoal and wood artifact, and at ~11,800 cal yr BP on peat soil, respectively (Jackson et al., 2007), demonstrating very low sedimentation rates. The peat is interpreted as organic deposition in a small pond, which is correlated upstream with a 5 cm thick layer of clay deposit (see Fig. 3, column C). This last observation suggests that the surrounding area would have been contemporaneously exposed to weathering and soil formation. The absence of alluvial deposits suggests a lack of

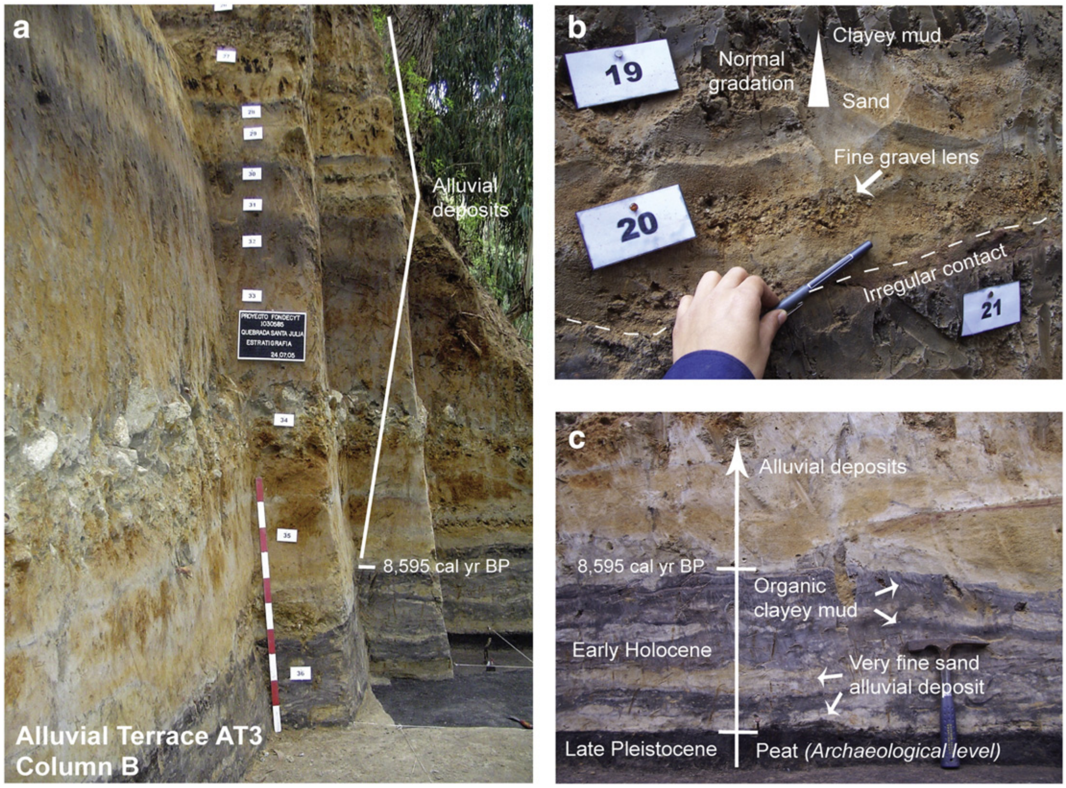

Figure 4. Photos of the sedimentological features of the alluvial terrace AT3 at Quebrada Santa Julia site (column B in Fig. 3).

Figure 5. Photos of the alluvial terraces AT2 and AT1. Location and sedimentological characteristics.

https://doi.org/10.1016/j.yqres.2012.08.002 Published online by Cambridge University Press

torrential rainfalls during the period of the black peat formation. In turn, the peat stratum suggests the occurrence of high humid conditions at the bottom of the local basin.

Fine dark-gray layers 45 cm thick overlay the peat. These consist of plastic clayey mud with high concentration of organic matter and scant alluvial deposits composed of very fine sand. This set finishes at ~8600 cal yr BP, according to radiocarbon dating from the highest clayey mud layer of this stratum (Fig. 4). The sedimentological characteristics of these deposits indicate a period of weak erosion in the ravine, suggesting therefore weak and scarce rainfall events. No evidences of roots, drying cracks or soil development were observed, indicating no or little hiatus in the alluvial sequence. Again, the organic matter content in these sediments suggests the development of local humid conditions concomitantly with the occurrence of weak and scarce rainfalls events.

The 9.5 m high sequence composed of debris and mud flows marks an important sedimentological change with respect to the underlying beds (Figs. 3 and 4). The sequence is composed of horizontally arranged sandy deposits with fine gravel lenses and normal grain-size gradation that rapidly alternate to clayey mud layers, with lower organic matter content on top, with respect to the strata constituting the underlying unit. These features point to a depositional environment where each alluvial deposit resulted from a single flood event, with quick deposition of sand and fine gravel followed by slower deposition of suspended mud including some development of organic soil probably related to remnant water at surface. Gravel lenses inside sandy facies indicate higher energy alluvial flows with respect to those with only sandy deposits (Fig. 4b). The deposits are characterized by irregular basal contacts and thickness of 20–80 cm. These textural characteristics together with subhorizontal arrangement of the deposits point to torrential rainfalls that produced mudflows that reworked sandy material already available in the watershed. This hydrologic pattern has driven alluvial aggradation along the whole local basin generating AT3. Because of less erosive distal alluvial environment most of the alluvium was accumulated and preserved at QSJ site. Five radiocarbon dates were obtained from five clayey mud layers of this unit. Once calibrated, these ages were used to interpret the frequency of alluvial episodes during the corresponding Holocene period (Fig. 6). The youngest age was obtained from the clayey mud close to the top of the stratigraphic column of AT3 (Méndez et al., 2007), indicating that this kind of alluvial flows occurred at least up to 2800 cal yr BP (Fig. 3).

After ~2800 cal yr BP, an incision process begun generating episodic downcutting throughout AT3; as the result of this, two lower alluvial terraces were formed inset (see Figs. 2c and 5). Terrace AT2 is ~2 m high, relative to the present thalweg of the ravine. The terrace is a 120 m long, 30 m wide alluvial surface characterized by slope of 1° toward the southwest, and consists of three debris-flow deposits. Terrace AT1 is ~1 m high, a 100 m long and 10 m wide alluvial surface, with a

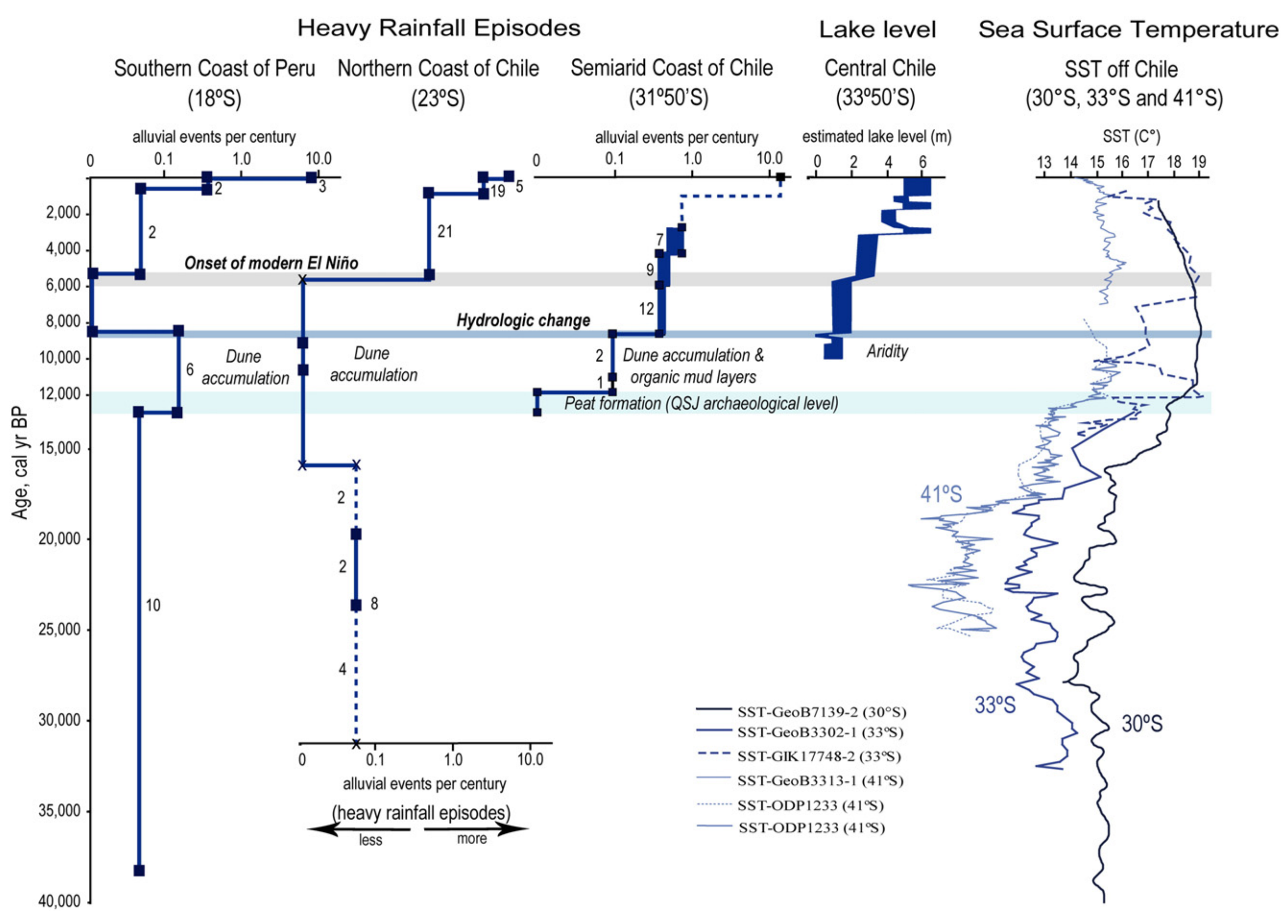

Figure 6. Comparison among heavy rainfalls episodes along subtropical west coast of South America, variations of Aculeo Lake level and sea surface temperature off Chile and Western Antarctic during latest Pleistocene and Holocene. Graphic of frequencies of alluvial events per century found at southern coast of Peru and northern coast of Chile were extracted from Vargas et al. (2006); frequencies of alluvial episodes at the semiarid coast of Chile (this work). Numbers at the side of each curve indicate the debris-flow events for the corresponding periods. Radiocarbon data are indicated by squares and extrapolated age estimates by crosses. Light blue horizontal bar shows peat formation period. Lake level changes from Laguna Aculeo of central Chile were extracted from Jenny et al (2002). Variations of the SST off Chile at 41°, 33°S and 30°S were extracted from Lamy et al. (2002, 2004, 2007), Kim et al. (2002), and Kaiser et al. (2005). Curves at 41°S and 33°S were recalibrated by Ortlieb et al. (2011). Dark blue horizontal bar indicates the major hydrologic change proposed in this work. Gray horizontal bar shows the onset of modern El Niño (Vargas et al., 2006). Horizontal bar thickness denotes the analytic errors of the geochronological model.

Table 2
Historical data regarding heavy rainfall associated to alluvial flows and flooding episodes at Coquimbo region during AD 1950–2000. The storms of July 11–16 and July 24 from 1987, and June 11–12 and June 18 and 21 from 1997 were considered as single events for NCEP/NCAR reanalysis.

No	Rainy event date	Rainfall	Duration[***]	Meteorological mechanism	Oceanic Niño index	Effects at La Serena surroundings (Coquimbo region)	Effects at Chile scale	References
1	1957, May 20–25	10.2 mm (May 20) and 60.2 mm (May 21) at La Serena[*] 203.6 mm (average for Coquimbo region)[**] Only monthly information available: 180.3 mm (May) at Puerto Oscuro[*]	5 days	Deep trough	0.7 (El Niño)	Great mud flow occurred on May 21 ranked one of the most catastrophic mud flows in history area. Cities full of mud and rocks. Elqui and Coquimbo rivers overflowed and devastated houses and everything in its path. La Serena and Coquimbo isolated. Small towns ravaged by rural ditches and streams. Wind and rain collapsed walls. Panamericana Highway cut into several large section. Hundreds of homeless.	The major storm affected central and northern Chile up to La Serena (30°S) 20 dead and 4 thousand homeless	El Día[**]: 1974 (June 10), 1983 (June 11), 1991 (June 23) Urrutia and Lanza 1993: 279–280
2	1965, August 9–10	27.5 mm (August 9), 36.5 mm (August 10) and 1.5 mm (August 11) at La Serena [*]	>17 hrs	Blocking	1.2 (El Niño)	Floods and landslides in whole province. Important roads and bridges cut by floods, e.g. Illapel–Los Vilos by Quebrada Canelillo and Illapel–Salamanca by Quebrada Lavaderos. Ports damaged by strong waves at Los Vilos and Pichidangui. Telegraph interrupted between La Serena and Santiago	48 h storm from southern region to Antofagasta in the north. 90% of country suffered damage by the storm Strong waves caused destruction in ports from Los Vilos (31°S) to Antofagasta (23°S)	El Día[**]: 1965 (August 10–12)
3	1972, June 13–14	37.2 mm (June 13) and 6.3 mm (June 14) at La Serena [*] 7.6 mm (June 13), 55 mm (June 14) and 1.2 mm (June 15) at Puerto Oscuro[*]	>6 h	Blocking	0.8 (El Niño)	Part of the highway and roads cut by floods in ravines and landslide (with mud and rocks) from the hills. Houses flooded. Train traffic to the north and south of La Serena stopped.	The storm affected two thirds of the country	El Día[**]: 1972 (June 13–15)
4	1972, August 24	66.7 mm (August 24) and 2.6 mm (August 25) at La Serena[*] 35 mm (August 25) and 1 mm (August 26) at Puerto Oscuro[*]	>12 h	Blocking	1.3 (El Niño)	Flooding and landslides. Trees fell down. Power lines cut. Traffic interrupted. Streets of La Serena city seemed like rivers. Roads of whole province were affected by the storm, except Panamericana Highway and paved roads. Intense snowfall at Elqui Valley, more than 4 m of snow at La Laguna dam. At Los Vilos, fishing boat ran aground due to rough seas and intense wind	The most intense and persistent storm since the mud flow of 1957	El Día[**]: 1972 (August 25–26)
5	1980, April 10–11	23.3 mm (April 10) and 2.1 mm (April 11) at La Serena[*] 80 mm (April 9) and 64 mm (April 10) at Puerto Oscuro[*]		Blocking	0.2 (Neutral)	Mud flow destroyed 30 m of asphalt Panamericana Highway (Punitaqui community). Three points of the Panamericana Highway between La Serena and Santiago cut off. Strong discharge in the ravines of the region. Houses flooded. Closure of ports. Strong northwest wind at Los Vilos. Roofs blown off in Ovalle, Illapel and Los Vilos	Strong storm (rain and wind) at Valparaíso (33°S) Homeless from Curicó (35°S) to La Serena (30°S) April 6, unexpected and heavy rainfall cut off roads in Atacama region (29 to 26°S)	El Día[**]: 1980 (April 9, 11–13)

6	1983, July 6–8	6.9 mm (July 6), 69.5 mm (July 7) and 40.4 mm (July 8) at La Serena[*] 51.5 mm (July 6), 39 mm (July 7) and 18.5 mm (July 8) at Puerto Oscuro[*]	~40 h	Blocking	0.2 (Neutral)	Thousands of homeless. Mud flow at Peñuelas and flood at Fundición Coquimbo. Bridges with pillars undermined by the force of the flow (e.g. Estero La Herradura). Roads cut by strong currents in the ravines of the region. Ten towns isolated in Coquimbo region. Loss of crops.	–	El Día[**]: 1983 (July 8–12)
7	1984, July 1–5 and 8–10	62.8 mm (July 1), 17 mm (July 2), 0.3 mm (July 3), 43.5 mm (July 4), 3.2 mm (July 5), 24.7 mm (July 8), 4.2 mm (July 9) and 21 mm (July 10) at La Serena[*] 23.2 mm (July 1), 10 mm (July 2), 88 mm (July 4), 20.5 mm (July 5), 30.3 mm (July 8), 12 mm (July 9) and 73.5 mm (July 10) at Puerto Oscuro[*]	~4 days	Deep trough → cutoff low	−0.3 (Neutral)	More than 35 thousand homeless in Coquimbo region. 9639 homeless in La Serena. The flow of Quebrada Arrayán swept 100 m of road and posts. Roads cut off and flooding in whole area. Mud and tailings flooded Andacollo. Craft stranded. Hundreds of sheep drowned in Elqui River. Snow up to 180 km east of the coast.	The storm affected a large part of Chile, from Punta Arenas (53°S) to Copiapó (27°S) Worst damage since 1957	El Día[**]: 1984 (July 2–17)
8	1987, July 11–16 and 24	5.8 mm (July 11), 26.9 mm (July 15) and 11.2 mm (July 16); 0.8 mm (July 23), 104.7 mm (July 24), 4.1 mm (July 25) at La Serena[*] 13.5 mm (July 10), 37.5 mm (July 11), 6 mm (July 12), 12 mm (July 13), 117 mm (July 14), 41 mm (July 15) and 6 mm (July 16); 17 mm (July 23), 59 mm (July 24) and 3.2 mm (July 25) at Puerto Oscuro[*]	3 days at La Serena (July 11–16) 7 days at Puerto Oscuro (July 10–16) ~ 12 h at La Serena (July 24) Unknown at Puerto Oscuro (July 24)	Deep trough → cutoff low	1.4 (El Niño)	(July 11–16) Almost two thousand homeless in Coquimbo region. Traffic stopped north of Santiago. Elqui River caused the isolation of Altovalsol town. Roads cut and suspended by strong currents in the ravines of the region as e.g. at Conchalí bridge at Los Vilos. July (24) More than eight thousand homeless at Coquimbo region. Three people dead. Serious road damage, deep fissures in roads.	More than 100 thousand homeless in whole Chile Serious damages in south of Coquimbo region. Extensive damage in the province of Huasco, southern Atacama region More than 100 thousand homeless in whole Chile	El Día[**]: 1987 (July 12–20; 25–30)
9	1991, June 16–19	9.6 mm (June 16), 42.9 mm (June 17), 4.5 mm (June 18) and 17.4 mm (June 19) at La Serena[*] 22.7 mm (June 16), 10 mm (June 18), 14 mm (June 19) and 25.7 mm (June 20) at Puerto Oscuro[*]	3 days	Blocking	0.8 (El Niño)	Rain and wind storm (30 km/h). Roads cut and bridges destroyed by strong currents in the ravines, transporting rocks and mud at Tongoy and Guanaqueros. 1116 homeless in Coquimbo region. Elqui River level rose sharply. Huasco River flooded some sectors. Towns isolated. Snow up to 90 km east of the coast. Almost 100 cm of snowfall at La Laguna.	Mud flows at Antofagasta, northern Chile (23°S), caused 20 thousand homeless and 80 died. Strong winds up 100 km/h at Tocopilla (22°S) Storm affected large part of Chile, from Rancagua (34°S) to Tocopilla (22°S) A cold front with post-front instability was reported by meteorologists on June 18	El Día[**]: 1991 (June 17–23)
10	1992, June 5–7	40.9 mm (June 5), 29.9 mm (June 6), 59.4 mm (June 7), 3 mm (June 8) at La Serena[*] 62.5 mm (June 5), 24 mm (June 6) and 35 mm (June 7) at Puerto Oscuro[*]	2 days	Cutoff low	0.8 (El Niño)	Mud flow caused deep cracks (up to 2 m) in streets because of flooding Jaramillo canal. Streets became rivers in Coquimbo. Strong winds destroyed roofs. Houses flooded. Power cut in Coquimbo. Strong winds at Los Vilos (up to 80 km/h). 150 miners isolated at Los Pelambres and also 40 in Salamanca.	Roads cut between Antofagasta (23°S) and Tocopilla (22°S) 500 miners isolated in Atacama region Storm affected from Puerto Montt (42°S) to Arica (19°S) during last days of May until the early days of June More than 27 thousand homeless in whole Chile 738% superavit of rainfall.	El Día[**]: 1992 (June 6–10) Urrutia and Lanza 1993: 394
11	1997, June 11–12 and 18 and 21	1.7 mm (June 10)[*], 26 mm (June 11)[*] and 32.2 mm (June 12)[*]; 11.6 mm (June 18)[**]and 17.5 mm	2 days (June 11–12) ~5 h (June 18)	Blocking	1.3 (El Niño)	(June 11–12) More than 4500 homeless in Choapa province. Electric storm, heavy rainfall and hail at	Storm affected a large part of Chile Heavy and persistent rainfalls at	El Día[**]: 1997 (June 12–14; 19–24)

(continued on next page)

Table 2 (*continued*)

No	Rainy event date	Rainfall	Duration[***]	Meteorological mechanism	Oceanic Niño index	Effects at La Serena surroundings (Coquimbo region)	Effects at Chile scale	References
		(June 21)[*] at La Serena 8.1 mm (June 11), 32.2 mm (June 12) and 34.2 (June 13); 1.2 mm (June 18), 11.8 (June 19), 2.3 mm (June 20) and 2.8 mm (June 21) at Puerto Oscuro[*]	~1 day (June 21)			Coquimbo. Mud flow at Guanaqueros (June 13). Flooding Elqui River swept riverside vegetation away. Houses flooded. Roads cut by strong mud flows. Gabriela Mistral international route cut off. Isolated families. Bridges in Elqui town destroyed. Snow up to 180 km east of the coast. (June 18–21) Mud flow at El Almendral (40 km east of La Serena) one and a half hour after the onset of rain. Vicuña town was isolated by strong discharge in San Carlos ravine. Main streets of Guanaqueros were destroyed by water and mud flows from the ravines. 15,300 homeless since the rainfall of June 11.	Coquimbo and Atacama regions (32°–26°S) –	
12	1997, August (16–18)	38.9 mm (onset at 18 h, August 16), 19 mm (August 17) and 5 mm (August 18) at La Serena[*] 15 mm (August 15), No data (August 16), 75.4 mm (August 17) and 31.6 mm (August 18)	~2 days	Blocking	2.0 (El Niño)	Torrential rainfall with strong wind (up to 100 km/h), sometimes intense but not persistent. Roads and bridges cut off by rivers and mud flows isolated towns, flooded houses and damaged agricultural crops. Strong wind brought down trees and caused severe damage in infrastructure, houses and boats. Closure of ports at Los Vilos, Tongoy and Guanaqueros. 50% of boats were destroyed at Guanaqueros.	Storm caused damage from Puerto Montt (42°S) to Coquimbo (30°S) Coquimbo region was most affected.	El Día[**]: 1997 (August 17–18)

[*] Meteorological data extracted from Dirección Meteorológica de Chile.
[**] Meteorological data extracted from El Día Newspaper.
[***] Duration corresponds to the length of rain at La Serena recorded by the newspaper El Día.

slope of 1° toward the southwest similar to the present thalweg of the ravine, and consists of one debris-flow deposit. Alluvial deposits forming both alluvial terraces have similar sedimentological features but are radically different relative to the alluvial deposits forming AT3 (Fig. 5). They are polymictic clast-supported gravel and ≤20 cm breccia, with sandy matrix, which directly overly the paleodune. Their strongly erosive basal contacts together with the occurrence of beds of gravel and sand that hold rock blocks, evidence vertical incision. These textural and stratigraphic features are interpreted as the result of debris flows with associated channelized and over-bank facies. The basal sediments and surface contact with the underlying dune deposits give evidence for basal shear plane development produced by high speed and energy of the alluvial flows. Although different sedimentological characteristics resulting from new geomorphologic conditions cannot be totally dismissed, the intensification of rainfall during the late Holocene and associated strong alluvial flows are probably the principal factors explaining the observed sedimentological features of AT1 and AT2.

Climate scenarios during modern heavy rainfalls and alluvial episodes

In austral summer the SEPSA, in combination with strong upslope regional-scale circulation, inhibit the development of a sea breeze through enhanced coastal subsidence in the afternoon (Rutllant et al., 2003). This prevents the inland development of convective cloudiness. During austral winter, this region is sporadically affected by convective rainfall associated with far-reaching, mid-latitude cold frontal disturbances and cut-off lows. Although rainfall can normally reach 30 mm/month, anomalously intense rainfall events have occasionally exceeded 200 mm in a few days. In settled weather, the stratus clouds that develop over the ocean below the subsidence inversion of the SEPSA can reach 1000 m altitude, favoring the development of coastal fogs and drizzle on the windward side of the coastal mountain range, especially during springtime when the extent of the low cloud deck is favored by low offshore sea-surface temperatures (e.g. Garreaud et al., 2008).

The occurrence of anomalous rainy years in central to northern Chile has commonly been associated with the development of El Niño conditions in austral winter–spring, arising from a weakened SEPSA (partially associated with negative Southern Oscillation Index values) and from a higher frequency/persistence of blocking anticyclones west of the Antarctic Peninsula (herein after BK mechanism). These anomalies result in an equatorward shift of storm tracks, allowing for cyclogenesis and frontal incursions off and along the central and north-central coast of Chile (Rutllant and Fuenzalida, 1991; Montecinos and Aceituno, 2003). Events occurring farther north (i.e. Antofagasta: ~23°S) in connection with El Niño have been explained by a combination of a weakened subsidence inversion (weaker SEPSA) and episodic warming of the coastal ocean which set the stage for the release of atmospheric potential instability during far-reaching mid-latitude frontal incursions and associated jet streams towards northern Chile. This mechanism may produce localized heavy convective storms, as in Antofagasta in 1991 (Garreaud and Rutllant, 1996).

One of the underlying hypotheses in this study is that the atmospheric circulation patterns conducive to modern debris-flow events could constitute analogs to explain the alluvial deposits found in the study area, given the geomorphologic framework of the Mal Paso creek. In order to assess these modern atmospheric circulation features, historical evidence of reported catastrophic debris flows associated with widespread rainfall episodes was collected from local newspapers. Beyond the study of the weather patterns associated with each of these episodes, it becomes relevant to know if all these strong rainfall events really produced debris flows in the study area, since previous soil moisture and rainfall intensity (convective cloudiness) are also important parameters, albeit difficult to obtain (e.g. Garreaud and Rutllant, 1996). Here we only consider heavy rainfall episodes that exceeded 32 mm at Puerto Oscuro and 20 mm La Serena, around one fourth and fifth of the annual average. However, most of them exceeded 50 mm and, exceptionally, there were events far in excess of 100 mm in both meteorological stations (e.g. the events of July 1983 and July 1984, Table 2).

By this approach, we documented 22 heavy precipitation events during AD 1950–2000 (Appendix table). Twelve of these events occurred in connection with El Niño, six under neutral ENSO conditions and four during La Niña. Meteorological conditions associated with each of these storms were assessed from 500 hPa (~5500 m asl) and 1000 hPa (near sea level) geopotential height anomaly charts from the NCEP/NCAR reanalysis (Kalnay et al., 1996), considering only the day with maximum precipitation within each event. Dominant anomaly patterns correspond to the BK mechanism (64%), in which anticyclonic anomalies are located to the SW of the South American continent around 90 W. These warm-core anticyclonic anomalies usually persist throughout the troposphere for a few days, blocking the westerly flow, resulting in an equatorward deviation of the storm tracks that produces cyclonic anomalies off subtropical Chile. This anomaly dipole, with negative (cyclonic) anomalies to over central Chile and positive (anticyclonic) ones west of the Antarctic peninsula, is a constituent of the Pacific South America (PSA) tropical-mid latitude teleconnection pattern identified by Mo and Higgins (1998). According to Rutllant and Fuenzalida (1991), these blocking episodes in the far SE Pacific occur normally during austral winter–spring, becoming more frequent during the developing phase

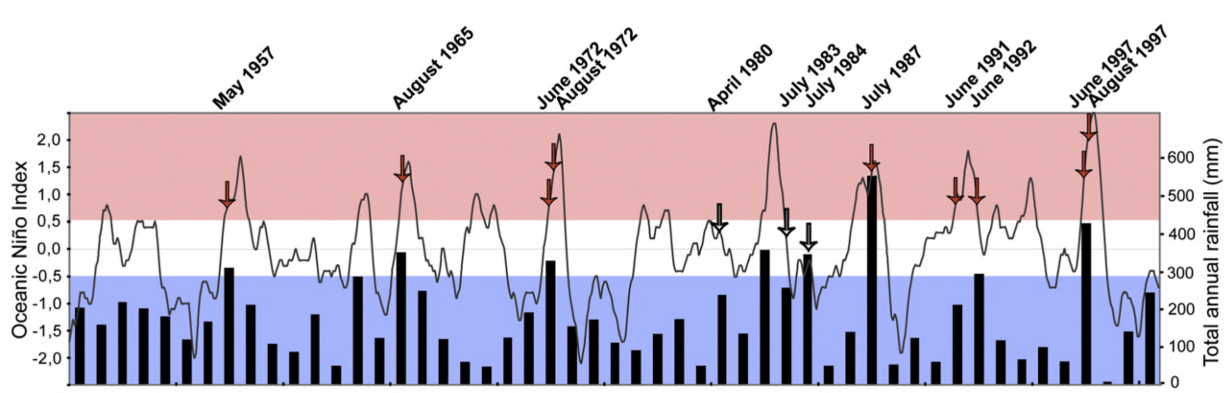

Figure 7. Rainy events that triggered debris flows or floods at semiarid coast of Chile (Coquimbo region) during AD 1950–2000, its relation with total annual rainfall at Puerto Oscuro and the Oceanic Niño Index. El Niño condition (red), neutral conditions (white), La Niña conditions (blue).

https://doi.org/10.1016/j.yqres.2012.08.002 Published online by Cambridge University Press

of El Niño events. The atmospheric circulation patterns in the remaining cases correspond to deep troughs (18%) stretching off and along the Chilean coast, and cutoff lows (9%). During extended rainfall periods a deep trough may evolve into a cutoff low when a high-pressure ridge overrides the trough in southern Chile, as occurred in July 1984 and 1987 (see Table in Appendix). Moreover, deep troughs may give rise to extended rainfall periods in north-central Chile when a blocking anticyclone develops east of the Andes over the South American cone (Garreaud, 1995). As documented in Fuenzalida et al. (2005), cutoff lows do not show a particular preference for any phase of the ENSO cycle.

Although the historical record may not be exhaustive due to newsworthiness, it indicates that at least twelve strong and regional rainfall events caused alluvial flows along the semiarid coast of Chile (Table 2, Fig. 7). Nine of these events occurred during the developing phase (austral winter) of El Niño, and the other three in neutral ENSO conditions. The latter correspond to events that occurred on April 10–11 of 1980, July 7–8 of 1983 and July 1–5 and 8–10 of 1984, which caused enormous damage (Table 2). Given that our sedimentological records at QSJ site features alluvial deposits prior to the onset of El Niño in the SE Pacific and in the west coast of South America (e.g. Rodbell et al., 1999) here we focus on the neutral ENSO phase assuming that this condition is representative of those that would have prevailed shortly after 8600 cal yr BP.

Hemispheric 500 hPa circulation anomaly patterns for the three catastrophic rainfall events in neutral ENSO conditions are depicted in Figure 8. The events of April 1980 and July 1983 occurred in connection with the aforementioned BK mechanism, while the July 1984 event resulted from a deep, slow-moving upper air trough along the Chilean coast and the subsequent formation of a cutoff low over north-central Chile. In this last case, the 500 hPa geopotential anomaly pattern resembles the BK one, except for positive (anticyclonic) anomalies to the SW of the negative one over central Chile (Fig. 8c). As mentioned before, in spite that the three circulation patterns are not alike, the negative (blue) anomalies across north-central Chile are very similar, including the trough axis (white dashed line). Figure 8 also illustrates the corresponding 500 hPa vector winds, indicating enhanced westerlies over central Chile. These results are consistent with those reported in Montecinos et al. (2011) as a non-ENSO signal typical of austral winter heavy rainfall episodes in central Chile, and with Garreaud (1995) who studied meteorological condition associated with heavy precipitation events in central Chile without any consideration of the phase of the ENSO cycle. From the nine debris-flow events that occurred under El Niño conditions, six correspond to the BK mechanisms, one occurred in connection with a deep trough, one with a cutoff low, and one with a deep trough evolving into a cutoff low (July 1987 event). Therefore, although the dominant mechanisms producing heavy rainfall episodes are alike for neutral and warm (El Niño) ENSO conditions, during the latter the BK mechanism is more frequent, as reported in Rutllant and Fuenzalida (1991).

Therefore, heavy rainfall episodes capable of producing alluvial events such as floods, debris and mud flows in north-central Chile can occur during El Niño and neutral ENSO conditions. In both scenarios, the cyclonic–anticyclonic meridional anomaly dipole seems to be a fundamental atmospheric circulation feature to drive frontal incursions toward lower latitudes. The enhanced westerlies over central Chile occurs when the polar jet merges with the subtropical one, in connection with the equatorward shift of the storm tracks associated with BK, deep quasi-barotropic troughs and subsequent cutoff lows.

Paleoclimatic implications

The sedimentary record from QSJ site points to a major hydrological regime shift during the early Holocene along the semiarid west coast of Chile. The development of peat in the absence of alluvial deposits during 13,000–11,800 cal yr BP suggests a lack of rainfall events, able to transport the available sand in the coastal watershed of the Mal Paso ravine, as well as local high moisture. The overlying strata composed by organic clayey mud as well as scant and fine alluvial deposits also suggest local moisture during 11,800–8600 cal yr BP, concomitantly with sporadic precipitation events that are able to transport very fine sand in the watershed. These stratigraphic data in combination with the analysis of the historical events might suggest La Niña-like conditions during the latest Pleistocene–early Holocene. The absence of torrential rainfalls can be explained by a strengthened SEPSA which could have favored high local moisture by intense and persistent coastal fogs.

Currently, coastal fogs are the main source of water for the relict forest of Fray Jorge National Park (Kummerow, 1966; del-Val et al., 2006), which is located 120 km north of QSJ site at 30°40′S. There, the maximum frequency of coastal fogs occurs during austral spring, when the temperature inversion is strong enough to confine the stratocumulus cloud deck over the subtropical Southeast Pacific (Garreaud et al., 2008) and the continental daytime heating is not extremely intense to foster cloud dissipation, as occurs during austral summer (Rutllant et al., 2003; Muñoz and Garreaud, 2007). During La Niña years, strengthening of the temperature inversion leads to a more persistent cloud deck and consequently higher than normal springtime fog frequency (Garreaud et al., 2008).

The sequence of alluvial deposits from QSJ site indicates a sharp increase in frequency and intensity of sporadic albeit torrential rainfall events shortly after 8600 cal yr BP, which suggests a major hydrological change along the semiarid coast of Chile relative to the previous early Holocene period. We propose that this sharp hydrological change resulted from a relatively reduced influence of the SEPSA along the subtropical Southeast Pacific, with respect to the early Holocene. This favored the occurrence of convective rainfall episodes concomitantly with regionally arid conditions, through climate mechanisms similar to those related with the occurrence of rainfalls over the semiarid coast of Chile during neutral ENSO years.

Farther north, alluvial deposits in southern Peru indicate heavy rainfall events between 12,900 and 8400 cal yr BP (Fig. 6), which were related to strong El Niño episodes at that period (Keefer et al., 1998, 2003). Subsequently, Vargas et al. (2006) associated the occurrence of those alluvial deposits to short and intense local heavy rainfall episodes during the winter–spring season along the coast of southern Peru, from enhanced low-level southerlies and orographic effect along the coastal range north of 18°S, where the coastline bends toward the northwest. This occurred with regionally intensified anticyclonic circulation and coastal upwelling which also inhibited the occurrence of strong alluvial episodes along the hyperarid coast of northern Chile, suggesting La Niña-like conditions during the latest Pleistocene and early Holocene (Vargas et al., 2006). A stronger SEPSA also inhibits the penetration of mid-latitude frontal systems towards the study area in the semiarid region, supporting the lack of torrential rainfall there. This hypothesis is consistent with reinforced coastal fogs along the subtropical coast (Garreaud et al., 2008) and, similarly to Fray Jorge forest (Kummerow, 1966; del-Val et al., 2006), explains typical taxa of humid environments found in pollen records at the QSJ site (Maldonado et al., 2010) and Palo Colorado, 24 km to the south (Maldonado and Villagrán, 2006), during the early Holocene. This climate scenario is also consistent with the development of black soils of up to 80 cm thick associated with relatively stable conditions along the semiarid coastal range surface (27° and 33°S) between 11,000 and 8160 cal yr BP (Veit, 1996). Intensified S-SW winds driven by the strengthened anticyclone would have favored the deposition of coastal dunes in Los Vilos area between 13,000 and 9550 cal yr BP (Fig. 6), like along the southern coast of Peru during 12,880–11,580 cal yr BP and northern Chile especially between 10,550 and 9124 cal yr BP (Vargas et al., 2006). This contrasts with the reduced influence of the southern westerly wind belt suggested in central-southern Chile during the early Holocene (Lamy et al., 2010), consistent with the extreme aridity prevailing in the Aculeo basin at 33°50′S before 8500 cal yr BP (Jenny et al., 2002).

The absence of alluvial deposits in southern Peru during 8400–5300 cal yr BP and the persistent lack of alluvial deposits

https://doi.org/10.1016/j.yqres.2012.08.002 Published online by Cambridge University Press

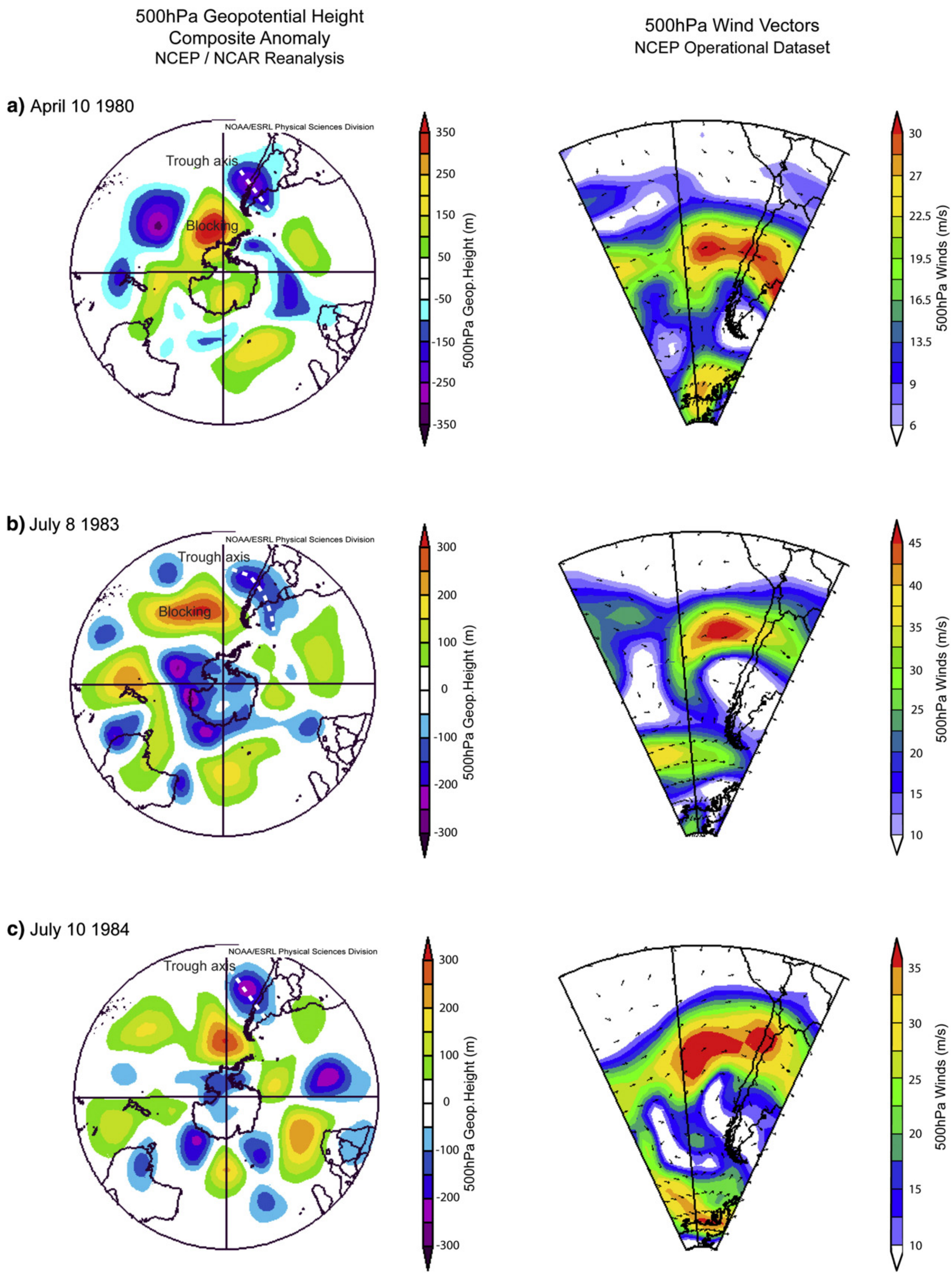

Figure 8. Composite anomalies of 500 hPa geopotential heights and wind vectors for three storm events that caused alluviums in neutral conditions according to ENSO cycle. The events correspond to: a) July 8, 1983; b) July 10, 1984 (http://www.esrl.noaa.gov/psd/data/histdata/).

along the coast of northern Chile (Keefer et al., 1998, 2003; Vargas et al., 2006; Fig. 6), suggest a decrease in the strength of the coastal southerlies along the coast of northern Chile and southern Peru as compared with the latest Pleistocene–early Holocene period (Vargas et al., 2006). Specifically, milder southerlies along northern Chile would not produce enough surface convergence in southern Peru to foster heavy rainfall events. Nevertheless, its influence would have been sufficient to prevent mid-latitude weather systems to penetrate the northern Chile coast, preserving aridity there. The hydrologic change suggested by the sedimentological record from QSJ site is concurrent with the onset of water accumulation in the Aculeo Lake (33°50′S) at 8500 cal yr BP (Fig. 6) when it became a more permanent shallow saline lake with carbonate precipitation (Jenny et al., 2002). Furthermore, the high content of *Chenopodiaceae* sp. and low content of arboreal pollen in the Aculeo record (Jenny et al., 2002), support overall conditions of aridity until 5700 cal yr BP, which is consistent with the pollen record from Palo Colorado (Maldonado and Villagrán, 2006) and with the preservation of paleosoils along the subtropical coastal region of Chile (Veit, 1996). Therefore, the absence of heavy rainfall events north of 30°S during 8400–5300 cal yr BP can be explained by the lack of ENSO tropical–extratropical climate teleconnection (Vargas et al., 2006), and generally reduced ENSO activity as suggested by other climate proxies from the eastern Pacific Ocean (Koutavas et al., 2006), from the western equatorial Andes (Rodbell et al., 1999; Moy et al., 2002), and from the Aculeo record in central Chile (Jenny et al., 2002).

Alluvial records from the western slope of the Andes support an onset of modern El Niño conditions including ENSO tropical–extratropical climate teleconnections at ca. 5500–5300 cal years BP (Rodbell et al., 1999; Vargas et al., 2006). The paleoclimate record of the QSJ site shows a slight increase in the frequency of alluvial episodes at that time, without significant sedimentological changes. This is probably due to the lower sensitivity of this proxy compared, for example, with the occurrence of alluvial episodes along the hyperarid coastal Atacama Desert of northern Chile and southern Peru (Vargas et al., 2006, Fig. 6), where heavy rainfalls were previously absent. The extraordinary heavy rainfalls responsible for historic disastrous alluvial events during the twentieth century in northern Chile have been associated with El Niño episodes, during which the PSA teleconnection wave train (Mo and Higgins, 1998) gets stronger or is located equatorward from its usual position, allowing for the entrance and further development of frontal systems at lower latitudes (Vargas et al., 2000, 2006). The onset of ENSO tropical–extratropical atmospheric teleconnection during the mid-Holocene is also consistent with the notable change from saline- to fresh-water conditions due to an increase in the Aculeo lake level, and with increased torrential clastic sedimentation since ca. 5700 cal yr BP (Jenny et al., 2002; Fig. 6), associated with torrential rainfall episodes in central Chile during modern El Niño (Rutllant and Fuenzalida, 1991). The notable sedimentological change of debris-flow deposits characterizing the lower terraces AT2 and AT1 in the Mal Paso ravine, with respect to the alluvial sequence forming AT3, together with the historic information (Table 2), suggests intensified alluvial episodes concomitantly with the incision of the hydrologic system during the late Holocene. This last inference agrees with intensified and higher frequency of alluvial events associated to El Niño during the last millennium and especially during the 20th century, deduced from the geomorphologic record from southern Peru and northern Chile (Vargas et al., 2006).

The paleoceanographic record off central-southern Chile shows that the period between 13,000 and 11,800 cal yr BP was characterized by regional SST warming trend during deglaciation times in the eastern boundary Humboldt Current System (Kim et al., 2002; Lamy et al., 2002, 2004, 2007; Kaiser et al., 2008; Ortlieb et al., 2011; Fig. 6). Cooler or similar than modern SSTs, together with an intensified Southeastern Pacific Subtropical Anticyclone associated with La Niña-like conditions, would have favored intensified coastal fog development off central-northern Chile during the latest Pleistocene and the beginning of the Holocene, as discussed earlier. The record off central Chile suggests a warming SST trend during the early to mid-Holocene transition, followed by a cooling trend during the late Holocene (Kim et al., 2002; Kaiser et al., 2008; Ortlieb et al., 2011). These paleoceanographic changes occurred roughly concomitantly with a high deglaciation rate of the Western Antarctic Ice Sheet during 12.6–10 cal ka BP, estimated from the western Amundsen Sea (Smith et al., 2011), and with a rapid landward recession of the Antarctic glaciers together with the onset of seasonal sea-ice formation which occurred around 8000–7800 cal yr BP (Finocchiaro et al., 2005). In this context, the change from higher to lower influence of the Southeast Subtropical Anticyclone on the semiarid coast of Chile at ca. 8600 cal yr BP occurred concomitantly with SST variations from relatively cooler to warmer conditions between the early to mid-Holocene period, especially off central Chile (Fig. 6), while the onset of modern ENSO during the mid-Holocene (Rodbell et al., 1999; Vargas et al., 2006) and the end of this oceanic trend are roughly contemporaneous.

Conclusions

The paleoclimate record from Quebrada Santa Julia site supports a major hydrologic change along the semiarid west coast of South America during the early Holocene. The sedimentological features of this record suggest an arid climate setting without torrential rainfalls, but with high local humidity due to reinforced coastal fogs between 13,000 and 8600 cal yr BP. The latter was associated with strengthened SEPSA and probably with cooler or similar than modern sea surface temperatures, similar to conditions of maximum frequency of coastal fogs that currently occur during austral spring and more intensely during La Niña years. The record of QSJ site supports intensified southerly winds, strengthened SEPSA and mean La Niña-like state during the early Holocene as suggested by dune accumulations along the western coast of South America (34°–18°S), heavy rainfall episodes deduced from alluvial records along the southern coast of Peru (18°S) and by the absence of them at the northern coast of Chile (23°S) (Vargas et al., 2006), together with an extremely low lake level in the Aculeo basin in central Chile (33°50′S) (Jenny et al., 2002). The QSJ archeological layer dated at 13000 cal yr BP (Jackson et al., 2007) developed under this regionally arid climate scenario was favored by local wet conditions associated with intensified coastal fogs and coastal geomorphology.

The notable frequency change deduced for the alluvial record of the QSJ site shortly after 8600 cal yr BP, suggests a new rainfall regime over the semiarid coast of Chile characterized by episodic and torrential rainfall events, which occurred still under an arid setting. We interpret that alluvial episodes associated with heavy rainfalls prior to 5700 cal yr BP resulted from relatively reduced influence of the SEPSA along the subtropical coast of Chile, with respect to the early Holocene, favoring the occurrence of sporadic convective rainfall events. According to modern meteorological analogs, these heavy rainfalls would have occurred under ocean-climate conditions similar to those characterizing neutral ENSO years, through the increase in large-scale westerlies flow over north-central Chile as suggested by Montecinos et al. (2011) and consistently with an equatorward shift of the Southeastern Pacific Subtropical Anticyclone.

Acknowledgments

This study was funded by FONDECYT 1090044 (DJ) and 11060484 (GV) grants and a CONICYT doctoral grant to CO. We thank the Department of Geology of University of Chile for laboratory facilities. Special thanks to Roxana Seguel for the field support. We thank Rene Garreaud, Fernando Sepúlveda, Carmina Jorquera and Jacobus Le Roux for their comments and fruitful discussions. Special thanks are also due to Editor Alan Gillespie, Associate Editor J. O'Connor and anonymous reviewers for constructive suggestions that contributed to a significant improvement of the manuscript. The authors gratefully acknowledge additional support from CEGA (Andean Geothermal Centre of Excelence), FONDAP project 15090013 (GV), and CEAZA (Center for Advanced Studies in Arid Zones) (JR).

Appendix A. Supplementary data

Supplementary data to this article can be found online at http://dx.doi.org/10.1016/j.yqres.2012.08.002.

References

Carré, M., Azzoug, M., Bentaleb, I., Chase, B.M., Fontugne, M., Jackson, D., Ledru, M., Maldonado, A., Sachs, J.P., Schauer, A.J., 2011. Mid-Holocene mean climate in the south eastern Pacific and its influence on South America. Quaternary International 253, 55–66.

del-Val, E., Armesto, J.J., Barbosa, O., Christie, D.A., Gutiérrez, A., Jones, C., Marquet, P., Weathers, K., 2006. Rain forest islands in the Chilean semiarid region: fog-dependency, ecosystem persistence and tree regeneration. Ecosystems 9, 1–13.

Finocchiaro, F., Langone, L., Colizza, E., Fontolan, G., Giglio, F., Tuzzi, E., 2005. Record of the early Holocene warming in a laminated sediment core from Cape Hallett Bay (Northern Victoria Land, Antarctica). Global and Planetary Change 45, 193–206.

Fuenzalida, H., Sanchez, R., Garreaud, R., 2005. A climatology of cut off lows in the Southern Hemisphere. Journal of Geophysical Research 110, D1801. http://dx.doi.org/10.1029/2005JD005934.

Garreaud, R., 1995. Configuraciones atmosféricas durante tormentas pluviales en Chile central. Meteorológica (Argentina) 19, 73–81.

Garreaud, R., Rutllant, J., 1996. Análisis meteorológico del los aluviones de Antofagasta y Santiago de Chile en el periodo 1991–1993. Atmosfera 9, 251–271.

Garreaud, R., Barichivich, J., Christie, D.A., Maldonado, A., 2008. Interannual variability of the coastal fog at Fray Jorge relict forests in semiarid Chile. Journal of Geophysical Research 113, G04011.

Grosjean, M., Núñez, L., Cartajena, I., Messerli, B., 1997. Mid-Holocene climate and culture change in the Atacama Desert, northern Chile. Quaternary Research 48, 239–246.

Heusser, C.J., 1990. Ice age vegetation and climate of subtropical Chile. Palaeogeography, Palaeoclimatology, Palaeoecology 80, 107–127.

Jackson, D., 1993. Datación radiocarbónica para una adaptación costera del Arcaico Temprano en el Norte Chico, Comuna de los Vilos. Boletín de la Sociedad Chilena de Arqueología 16, 28–31.

Jackson, D., 2002. Cazadores y recolectores del Holoceno Medio del norte semiárido de Chile. Tesis para optar al grado de Magíster en Arqueología. Universidad de Chile. Ms.

Jackson, D., 2003. Evaluating evidence of cultural associations of Mylodon in the semiarid region of Chile. In: Miotti, L., Salemme, M., Flegenheirmer, N. (Eds.), Where the South Winds Blow, Ancient evidence of Paleo South Americans. Center for the Study of the First Americans, College Station, pp. 77–81.

Jackson, D., Méndez, C., 2005. Primeras ocupaciones humanas en la costa del semiárido de Chile: patrón de asentamientos y subsistencia. Actas del XVI Congreso Nacional de Arqueología Chilena, pp. 493–502.

Jackson, D., Méndez, C., Seguel, R., Maldonado, A., Vargas, G., 2007. Initial occupation of the Pacific Coast of Chile during late Pleistocene times. Current Anthropology 48, 725–731.

Jenny, B., Valero-Garcés, B.L., Villa-Martinez, R., Urrutia, R., Geyh, M.A., Veit, H., 2002. Early to mid-Holocene aridity in central Chile and the southern westerlies: the Aculeo Lake record (34°S). Quaternary Research 58, 160–170.

Jenny, B., Wilhelm, D., Valero-Garcés, B.L., 2003. The southern westerlies in central Chile: Holocene precipitation estimated based on a water balance model for Laguna Aculeo (33°50′S). Climate Dynamics 20, 269–280.

Kaiser, J., Lamy, F., Hebbeln, D., 2005. A 70-kyr sea surface temperature record off southern Chile (ocean drilling program site 1233). Paleoceanography 20, PA4009. http://dx.doi.org/10.1029/2005PA001146.

Kaiser, J., Schefuss, E., Lamy, F., Mohtadi, M., Hebbeln, D., 2008. Glacial to Holocene changes in sea surface temperature and coastal vegetation in north central Chile: high versus low latitude forcing. Quaternary Science Reviews 27, 2064–2075.

Kalnay, et al., 1996. The NCEP/NCAR 40-year reanalysis project. Bulletin of the American Meteorological Society 77, 437–470.

Keefer, D.K., deFrance, S.D., Moseley, M.E., Richardson III, J.B., Satterlee, D.R., Day-Lewis, A., 1998. Early maritime economy and El Niño events at Quebrada Tacahuay, Perú. Science 281, 1833–1835.

Keefer, D.K., Moseley, M.E., deFrance, S.D., 2003. A 35,000-year record of floods and debris flows in the Ilo region of southern Peru and its relation to El Niño events and great earthquakes. Palaeogeography, Palaeoclimatology, Palaeoecology 194, 41–77.

Kim, J.-H., Schneider, R.R., Hebbeln, D., Müller, P.J., Wefer, G., 2002. Last deglacial sea-surface temperature evolution in the Southeast Pacific compared to climate changes on the South American continent. Quaternary Science Reviews 21, 2085–2097.

Koutavas, A., de Menocal, P.B., Olive, G.C., Lynch-Stieglitz, J., 2006. El Niño-Southern Oscillation (ENSO) attenuation revealed by individual foraminifera in eastern tropical Pacific sediments. Geology 34, 993–996.

Kummerow, J., 1966. Aporte al conocimiento de las condiciones climáticas del bosque de Fray Jorge. Boletín Técnico, Facultad de Agronomía Universidad de Chile 24, 21–24.

Lamy, F., Hebbeln, D., Wefer, G., 1999. High-resolution marine record of climatic change in mid-latitude Chile during the last 28,000 years based on terrigenous sediment parameters. Quaternary Research 51, 83–93.

Lamy, F., Rühlemann, C., Hebbeln, D., Wefer, G., 2002. High- and low-latitude climate control on the position of the southern Peru–Chile current during the Holocene. Paleoceanography 17 (2), 1028. http://dx.doi.org/10.1029/2001PA000727.

Lamy, F., Kaiser, J., Ninnemann, U., Hebbeln, D., Arz, H., Stoner, J., 2004. Antarctic timing of surface water changes off Chile and Patagonian Ice Sheet response. Science 304, 1959–1962.

Lamy, F., Kaiser, J., Arz, H.W., Hebbeln, D., Ninnemann, U., Timm, O., Timmermann, A., Toggweiler, J.R., 2007. Modulation of the bipolar seesaw in the Southeast Pacific during termination 1. Earth and Planetary Science Letters 259, 400–413.

Lamy, F., Kilian, R., Arz, H.W., Francois, J., Kaiser, J., Prange, M., Steinke, T., 2010. Holocene changes in the position and intensity of the southern westerly wind belt. Nature Geoscience 3, 695–699.

Maldonado, A., Villagrán, C., 2006. Climate variability over the last 9900 cal yr BP from a swamp forest pollen record along the semiarid coast of Chile. Quaternary Research 66, 246–258.

Maldonado, A., Méndez, C., Ugalde, P., Jackson, D., Seguel, R., Latorre, C., 2010. Early Holocene climate change and human occupation along the semiarid coast of north-central Chile. Journal of Quaternary Science 25, 1–4.

Méndez, C., Jackson, D., Seguel, R., 2007. Current evidence and radiocarbon chronology from Santa Julia late Pleistocene settlement in the semiarid coast of Chile (31°50′S). Current Research in the Pleistocene 24, 68–69.

Mo, K.C., Higgins, R.W., 1998. The Pacific South American modes and tropical convection during the southern hemisphere winter. Monthly Weather Review 126, 1581–1596.

Montecinos, A., Aceituno, P., 2003. Seasonality of the ENSO-related rainfall variability in central Chile and associated circulation anomalies. Journal of Climate 16, 281–296.

Montecinos, A., Kurgansky, M.V., Muñoz, C., Takahashi, K., 2011. Non-ENSO rainfall variability in central Chile during austral winter. Theoretical and Applied Climatology 106, 557–568.

Moy, C.M., Seltzer, G.O., Rodbell, D.T.Y., Anderson, D.M., 2002. Variability of El Niño/Southern Oscillation activity at millennial timescales during the Holocene epoch. Nature 420, 162–165.

Muñoz, R., Garreaud, R., 2007. The coastal boundary layer diurnal cycle along north central Chile: observations and model sensitivities. 7th Conference on Coastal Atmospheric and Ocean Prediction and Processes, American Meteorological Society, San Diego, California, 10–13 Sept.

Ortlieb, L., Vargas, G., Saliège, J.F., 2011. Marine radiocarbon reservoir effect along the northern Chile–southern Peru coast (14–24°S) throughout the Holocene. Quaternary Research 75, 91–103.

Reimer, P.J., Baillie, M.G.L., Bard, E., Bayliss, A., Beck, J.W., Bertrand, C., Blackwell, P.G., Buck, C.E., Burr, G., Cutler, K.B., Damon, P.E., Edwars, R.L., Fairbanks, R.G., Friedrich, M., Guilderson, T.P., Hughen, K.A., Kromer, B., McCormac, F.G., Manning, S., Bronk Ramsey, C., Reimer, R.W., Remmele, S., Southon, J.R., Stuiver, M., Talamo, S., Taylor, F.W., van der Plicht, J., Weyhenmeyer, C.E., 2004. IntCal04 terrestrial radiocarbon age calibration, 0–26 cal kyr BP. Radiocarbon 46, 1029–1058.

Rodbell, D.T., Seltzer, G.O., Anderson, D.M., Abott, M.B., Enfield, D.B., Newman, J.H., 1999. An ~15,000-year record of El Niño-driven alluviation in southwestern Ecuador. Science 283, 516–520.

Roman, A., Jackson, D., 1998. Dataciones por termoluminicencia de rocas de fogones de asentamientos arcaicos, Provincia del Choapa. Chungará 30, 41–48.

Rutllant, J., Fuenzalida, H., 1991. Synoptic aspects of the central Chile rainfall variability associated with the Southern Oscillation. International Journal of Climatology 11, 63–76.

Rutllant, J., Fuenzalida, H., Torres, R., Figueroa, D., 1998. Interacción océano-atmósfera-tierra en la Región de Antofagasta (Chile, 23°S): Experimento DICLIMA. Revista Chilena de Historia Natural 71, 405–427.

Rutllant, J., Fuenzalida, H., Aceituno, P., 2003. Climate dynamics along the arid northern coast of Chile: the 1997–1998 Dinámica del Clima de la Región de Antofagasta (DICLIMA) experiment. Journal of Geophysical Research 108, 4538.

Sandweiss, D.H., Richardson, J.B., Reitz, E.J., Rollins, H.B., Maasch, K.A., 1996. Geoarchaeological evidence from Peru for a 5000 years BP onset of El Niño. Science 273, 1531–1533.

Smith, J.A., Hillenbrand, C., Kuhn, G., Larter, R.D., Graham, A.G.C., Ehrmann, W., Moreton, A.G., Forwick, M., 2011. Deglacial history of the West Antarctic Ice Sheet in the western Amundsen Sea embayment. Quaternary Science Reviews 30, 488–505.

Strub, T., Mesías, J., Montecino, V., Rutllant, J., Salinas, S., 1998. Coastal ocean circulation off western South America. In: Robinson, Allan R., Brink, Kenneth H. (Eds.), The Sea, 11, pp. 273–313.

Urrutia, R., Lanza, C., 1993. Catástrofes de Chile: 1541–1992. Editorial La Noria, Santiago, Chile.

Vargas, G., Ortlieb, L., Rutllant, J., 2000. Aluviones históricos en Antofagasta y su relación con eventos El Niño/Oscilación del Sur. Revista Geológica de Chile 27, 157–176.

Vargas, G., Rutllant, J., Ortlieb, L., 2006. ENSO tropical–extratropical climate teleconnections and mechanisms for Holocene debris flows along the hyperarid coast of western South America (17°–24°S). Earth and Planetary Science Letters 249, 467–483.

Veit, H., 1996. Southern westerlies during the Holocene deduced from geomorphological and pedological studies in the Norte Chico, northern Chile (27–33°S). Palaeogeography, Palaeoclimatology, Palaeoecology 123, 107–119.

Villagrán, C., Varela, J., 1990. Palynological evidence for increased aridity on the central Chilean coast during the Holocene. Quaternary Research 34, 198–207.

Villa-Martínez, R., Villagrán, C., Jenny, B., 2003. The last 7500 cal yr BP of westerly rainfall in central Chile inferred from a high-resolution pollen record from Laguna Aculeo (34°S). Quaternary Research 60, 284–293.